

## Experimental observation of inter-ELM filaments in MAST

N. Ben Ayed<sup>1,2</sup>, A. Kirk<sup>2</sup>, B. Dudson<sup>1</sup>, R. G. L. Vann<sup>1</sup>, S. Tallents<sup>2</sup>,

H. R. Wilson<sup>1</sup> and the MAST team.

<sup>1</sup> Department of Physics, University of York, Heslington, York, YO10 5DD, U.K.

<sup>2</sup> UKAEA Fusion Association, Culham Science Centre, Abingdon, Oxfordshire, U.K.

### 1. Introduction

Filamentary structures are a ubiquitous feature of the edge cross-field transport in the boundary of magnetically confined plasmas. Efforts have so far concentrated on the characterisation of edge L-mode and ELM structures. As a result, our understanding of the transport related phenomena in inter-ELM periods is still limited. In this contribution, experimental results on edge turbulence during inter-ELM periods in MAST will be presented, and compared with those of L-mode and ELM results. Combined measurements of fast camera images and reciprocating Langmuir probes provide new evidence for the filamentary nature of the transport during these periods.

### 2. Fast camera imaging

The visible light (mostly  $D_\alpha$ ) from the MAST edge is imaged with high temporal and spatial resolution using a fast camera (full frame @7500 f.p.s, partial frames @ $10^5$  f.p.s). Background subtraction techniques reveal field-aligned filamentary structures which exist during H-mode inter-ELM periods (see figure 1 (a)). By fitting EFIT-calculated field lines [1] to the 2D images, filaments are subsequently located and a comparison of the light intensity corresponding to filaments during inter-ELM (blue), L-mode (red) and ELM phases is made. Results are shown in figure 1 (d,e).

While Inter-ELM filaments are found to be the weakest fluctuations in the MAST scrape-off layer (SOL), the light emission of L-mode is twice that of inter-ELM, and both are much smaller than the stronger ELM disturbance. Taking into account field line pitch and blurring due to filament rotation, toroidal widths (in the direction perpendicular to the field-line) of inter-ELM filaments have been obtained from the width of their corresponding peaks in  $D_\alpha$  emission. Peak (most likely) values are found to be in the range 10 – 11.5 cm while peak toroidal spacings are  $\sim 15$  cm.

The spatiotemporal evolution of inter-ELM filaments is also described by fitting field lines to filaments in sequential frames. Filaments in the vicinity of the last closed flux surface (LCFS) are found to rotate with toroidal velocities in the range 3 – 12.5 km/s. It is also found that whereas toroidal velocity for any given filament is on average constant, the collective motions of filaments is more complex: filaments are not regularly spaced, and due to different toroidal velocities, their spacing's are constantly changing. It is for this reason that inter-ELM quasi mode numbers vary over a large range, 10–40, with peak value  $\sim 22$ . In addition to toroidal rotation, filaments are also observed to propagate radially outwards beyond the immediate SOL. See [2,3] for examples of this motion. Typical radial velocities are in the range 1–2 km/s.

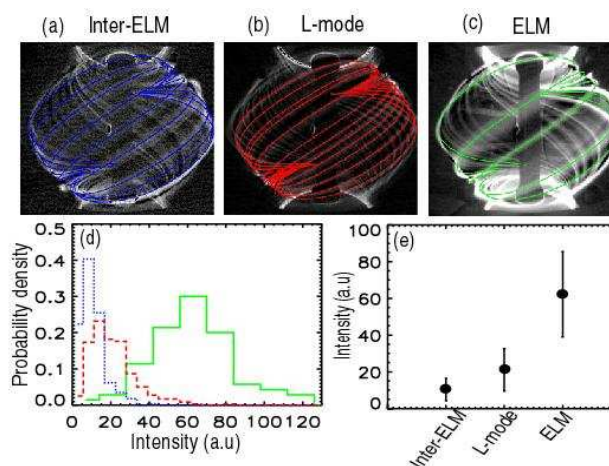


**Figure 1** Full view images with background subtraction of (a) inter-ELM (blue), (b) L-mode (red) and (c) ELM (green) phases; (d) PDFs of light intensity of filaments and (e) mean intensity values.

In order to investigate any dependence of filament motion on plasma parameters, toroidal and radial displacements of filaments have been tracked over a wide variety of parameters involving the

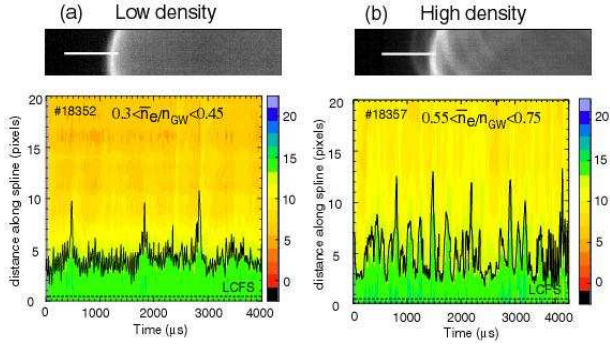


**Figure 3** Colour plots of intensity along white line as a function of time and distance in pixels.

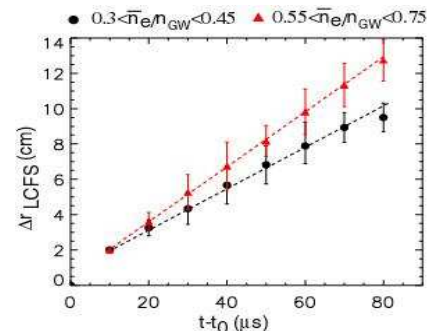
number of filaments which leave the edge of the plasma, and hence an enhancement of the radial transport. The radial position from the LCFS of these filaments has also been tracked as a function of time for high and low density discharges. As shown in figure 3, filaments are tracked for periods up to 80  $\mu\text{s}$ , and to distances in the range 10–12 cm from the LCFS before they disintegrate due to parallel transport. During this time, there is no evidence to suggest that filaments accelerate away from the edge: For both high and low  $\bar{n}_e$ , linear fits corresponding to a constant radial velocity give a good description of the data. Furthermore, filaments in high density discharges expand on average faster than filaments at low density. Mean radial velocities are  $\sim 1.65$  km/s and 1.2 km/s respectively for high and low densities.

### 3. Langmuir probe

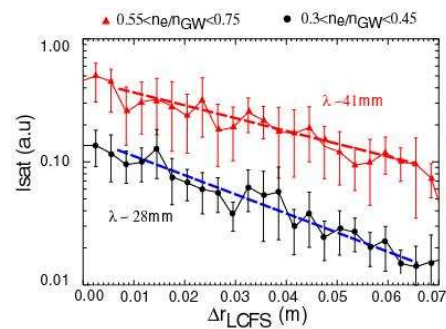
Inter-ELM filaments have been characterised by the outboard midplane reciprocating system on MAST. This consists of a circular array of 8 equally spaced Langmuir probes arranged in opposite pairs, and biased to -220V to measure the ion saturation current,  $I_{\text{sat}}$ . It was shown with the aid of the camera that intermittent fluctuations in ion saturation current signals correspond to filaments passing the probe [1,2]. Typical  $I_{\text{sat}}$  values corresponding to these structures have been used to infer a density for inter-ELM filaments which is in the range  $5 \times 10^{17} - 2 \times 10^{18} \text{ m}^{-3}$ .

Figure 4 shows on a log-linear scale the measured values of  $I_{\text{sat}}$  as a function of distance from the LCFS at high and low  $\bar{n}_e$ . Linear fits from 1–6 cm from the LCFS are shown by the dashed lines. The fits yield particle e-folding lengths of  $\lambda_{\text{high}} \sim 41\text{mm}$  at high  $\bar{n}_e$ , and  $\lambda_{\text{low}} \sim 28$  mm at low  $\bar{n}_e$ . Monte-Carlo simulations, described in [4,5], are performed in which a filament is assumed to propagate radially outwards with a velocity  $V_r$  and lose particles on the parallel loss time scale  $\tau_{\parallel} = L_{\parallel}/C_s$  (where  $L_{\parallel}$  is the connection length and  $C_s$  is the ion sound speed). Two simulations are performed with initial radial

line-averaged density  $\bar{n}_e$ , toroidal field  $B_{\phi}$ , plasma current  $I_p$  and neutral beam heating power  $P_{\text{NBI}}$ . Whilst no significant changes are observed with  $B_{\phi}$ ,  $I_p$  and  $P_{\text{NBI}}$ , motion of these filaments has been found to have a strong dependence on plasma density. Figure 2 shows a colour plot of the intensity as a function of distance along the spline (marked by the white line on the midplane images) and time. At higher  $\bar{n}_e$ , there is an increase in the



**Figure 2** Radial distance of filaments from LCFS as a function of time at high and low densities.



**Figure 4** Log-linear plot of  $I_{\text{sat}}$  values as a function of distance from the LCFS at high and low density.

velocities of 1.65 and 1.2 km/s respectively. An ion temperature of 30 eV is also assumed for both cases. The radial distribution of  $I_{sat}$  at the mid-plane is shown in figure 5 and is in excellent agreement with the experimental data. The filament which travels at 1.65 km/s, representative of the high density scenario, has a higher  $\lambda_{high} \sim 40$  mm than the filament in the low density scenario where  $\lambda_{low} \sim 30$  mm.

The mechanisms underlying the radial motion of filamentary structures in the SOL have been addressed by several theories. The curvature and non-homogeneity of the magnetic fields in these models result in charge-dependent guiding centre drifts of particles.

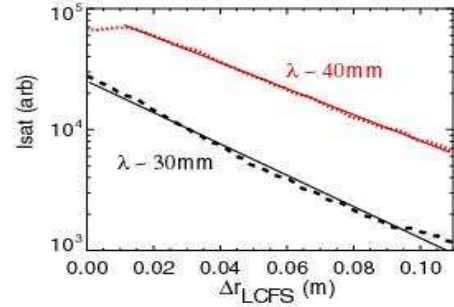


Figure 5 The radial distribution of  $I_{sat}$  at the midplane for two simulated filaments moving with constant radial velocities of 1.65 and 1.2

A first model is the sheath dissipative regime and is based on the assumption of electrostatic sheaths at divertor target plates. An analytical solution for the radial velocity is given by [6]:

$$\frac{V_r}{C_s} = \left( \frac{\rho_i}{L_{\perp}} \right)^2 \frac{L_{\parallel} n_f}{R n_t}$$

where  $n_f$  is the filament's density,  $n_t$  is the plasma density near the targets,  $C_s = \sqrt{T/M}$  is the plasma sound speed,  $M$  is the ion mass,  $\rho_i$  is the ion-gyro radius,  $L_{\perp}$  is the filament perpendicular size. A second model is the interchange regime and relies on the interchange drive due to the effective buoyancy of the plasma in a non-uniform magnetic field. The scaling for the maximum radial velocity takes the expression [7] :

$$\frac{V_r}{C_s} = \left( \frac{2L_{\perp} n_f}{R n_s} \right)^{0.5}$$

The quantities  $L_{\perp}$ ,  $L_{\parallel}$ ,  $C_s$  and  $n_{SOL}$  were found to be constant for the set of high and low density discharges considered. Hence, the predictions for the ratio of the velocities at high and low density can be expressed as:

$$\frac{V_r^{high}}{V_r^{low}} \sim \left( \frac{n_f^{high}}{n_f^{low}} \right)^{\alpha} \sim \left( \frac{I_{sat}^{high}}{I_{sat}^{low}} \right)^{\alpha}$$

where the  $\alpha$  exponent would equal 0.5 and 1 for the set of interchange and sheath scalings

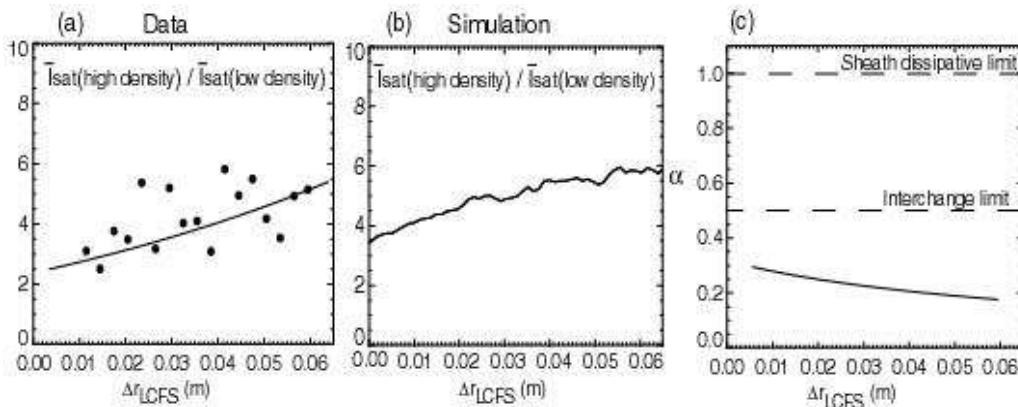


Figure 6 (a,b) Ratio of experimentally measured and simulated  $I_{sat}$  values at high and low density, and (c)  $\alpha$  exponent as a function of distance from the LCFS. Experimental values of  $\alpha$  lie below both sheath and interchange limits.

respectively. Figure 6 shows the ratio of the measured  $I_{sat}$  values at high and low  $\bar{n}_e$ , binned as a

function of distance from the LCFS. The solid line is the exponential fit obtained from the particle e-folding lengths estimated earlier. Monte-Carlo simulations of the ratio of  $I_{sat}$  signals also yield a similar trend, as shown in figure 6 (b).

The difficulty which arises when relating to predicted velocity scaling is immediately apparent since the ratio of the  $I_{sat}$  values is not constant as a function of distance from the LCFS. Taking  $V_r=1.65$  km/s, and  $V_r=1.2$  km/s, the  $\alpha$  exponent, shown in figure 6 (c), is given by the expression:

$$\alpha \sim 0.28 \log \left( \frac{I_{sat}^{high}}{I_{sat}^{low}} \right)^{-1}$$

Experimental values of alpha decrease from 0.3 in the proximity of the LCFS to 0.2 approximately 6cm from the edge, and are therefore factors of 4 and 2 smaller than sheath and interchange limits respectively. We conclude that neither model agrees with experiment.

#### 4. Conclusions and Summary

Results on edge turbulence during inter-ELM periods in MAST are presented. It is shown through combined measurements based on fast camera images and reciprocating Langmuir probes that filamentary structures influence the transport during these periods. A comparison of the  $D_\alpha$  light emission amplitudes reveals that inter-ELM filaments are the lowest fluctuations in the MAST SOL relative to L-mode and ELM filaments. Physical properties such as size, density and mode numbers have also been characterised, along with measurements of the spatio-temporal evolution: Inter-ELM filaments are found to rotate in the vicinity of the LCFS, and propagate radially outwards. Motion of these filaments is found to depend strongly on plasma density such that with increasing density, there is an enhancement of the radial transport which is clearly manifested by an increased number of filaments which leave the edge and travel faster into the SOL. With the aid of camera images, it is shown that intermittent fluctuations in ion saturation current signals correspond to inter-ELM filaments passing the probe. Measured radial e-folding lengths indicate higher fall-offs at higher densities. Similar trends are also obtained in Monte-Carlo simulations of a filament propagating radially and losing particles on ion parallel loss timescales. Finally, a discussion is presented on how the radial velocity and  $I_{sat}$  measurements have been used to test the predictions made by different models. The scalings observed in the data are at least a factor of 2 smaller than the models. In fact, the scalings have been found to vary as a function of distance in the SOL – a feature which is not captured in either model.

#### 5. References

- [1] Lao L. L., et al, 1985, *Nuclear Fusion*, **25**:1611-22.
- [2] Ben Ayed N., Kirk A., Dudson B., Tallents S., Vann R. L. Vann, Wilson H., submitted to *PPCF* 2008.
- [3] Ben Ayed N, et al, "Structure and motion of inter-ELM filaments", 34<sup>th</sup> EPS Conference, Warsaw, 2007.
- [4] Kirk A., et al, 2008, "Comparison of the filaments behaviour observed during type-I ELMs in ASDEX Upgrade and MAST", *J. of Phys.*, - conference series (IOP), accepted for publication.
- [5] Kirk A., et al, 2008, "Comparison of the spatial and temporal structure of type- I-ELMs " *J. Of Phys.*, - conference series (IOP), accepted for publication.
- [6] D'ippolito D. A. and Myra J. R., 2003, *Phys .of Plasmas*, **10**, 4029-39.
- [7] Garcia O. E., Bian N. H. and Fundamenski W., 2006, *Phys .of Plasmas*, **13** 082309.

*This work was funded in part by the United Kingdom Engineering and Physical Sciences Research Council and by EURATOM. The views and opinions expressed here-in do not necessarily reflect those of the European Commission.*